

A Comparison of Heat Pump and Resistive Heating Impacts on Battery Electric Vehicle Energy Consumption and Range in Cold Temperatures

Kieran Humphries¹ and Aaron Loiselle-Lapointe¹

¹*Transportation Emissions and Electrification Laboratory, Environment and Climate Change Canada,
335 River Road, Ottawa, ON, Canada, aaron.loiselle@ec.gc.ca*

Executive Summary

This paper presents the results from in-lab chassis dynamometer testing of two battery electric vehicles of the same make and model: a 2022 model year vehicle with a heat pump, and a 2020 model year vehicle with a resistive PTC heater. The vehicles were tested for energy consumption and range at a series of different temperatures over the same test procedure. The results indicate that in most (but not all) heating situations the heat pump was more efficient than the conventional PTC heater, especially at moderate temperature (0°C). The improvement in the percentage of driving range retained by the heat pump equipped vehicle over the PTC heater equipped vehicle varied between 1% and 15% depending on ambient conditions and drive cycle, with the average advantage in retained percentage range being 7% over the UDDS cycle, 7% over the HWFET cycle, and 4% over the US06 cycle.

Keywords: Electric Vehicles, Thermal Management, Energy Management

1 Introduction

Battery electric vehicles (BEV) operating in cold conditions are at an inherent disadvantage when compared to conventional internal combustion engine (ICE) vehicles, as they do not have a readily available source of waste heat with which to heat their cabin. ICE vehicles produce a significant amount of waste heat while driving, and this allows them to heat their cabin in cold conditions without using much additional stored energy (fuel) to do so. On the other hand, battery electric vehicle drivetrains are extremely efficient and do not produce much waste heat that could be used for heating, therefore requiring additional stored electrical energy to be used for their cabin heating, lowering electric vehicles' efficiency and driving range [1]. Historically, electric vehicles have used resistive elements for cabin heating in cold weather, which convert stored battery energy to heat directly. Resistive heating options include Positive Temperature Coefficient (PTC) type heaters positioned directly inside cabin ventilation ducts and liquid coolant heaters that provide heated coolant to a heater core within these ducts. In either case, resistive heaters can draw a significant load from the battery under cold ambient conditions, leading to high energy use and lowered vehicle driving range. To reduce cabin heating energy use, an increasing number of manufacturers are turning to the use of heat pump technology for their electric vehicles in cold climates [1]. Several electric vehicles offered in Canada include heat pump systems as standard (even if they would be considered optional equipment elsewhere), and some others include them as an option on certain trim levels. This study aims to compare the heating loads, energy consumption, and associated range loss when using resistive heating and heat pump systems for cabin heating at cold temperatures.

The test specimens chosen for this program were two Tesla Model 3 vehicles of different model years. Tesla's Model 3 has gone through several modifications over its production run, including a significant update to its heating system in 2021. Early versions of the vehicle use a dedicated PTC heater for cabin heating. This heater is located directly in the incoming cabin air stream and heats the air prior to it exiting the ventilation vents. A model update in 2021 saw the inclusion of an advanced heating system which uses a heat pump and additional hardware to create a complex heating system with many operating modes. These modes allow the heat pump to be used to scavenge heat from the ambient air (as is typical of an air-source heat pump system) and to use waste heat from some of the vehicle's components [2, 3]. In addition, as detailed in the manufacturer's patent filings, the heat pump system can run in a so-called "lossy mode" when temperatures are very cold, which allows it to produce heat directly using the heat pump compressor (avoiding the need for a backup PTC heater, unlike most other electric vehicle models with heat pump systems) [2, 3]. The substantial modifications to this vehicle model's heating system between model years offers a unique opportunity to compare the cold weather performance of similar electric vehicles with and without a heat pump system.

2 Methods

In the fall of 2022, the two test vehicles were tested over the same chassis dynamometer test procedures at the Transportation Emissions and Electrification Laboratory in Ottawa, Canada. The procedure followed the Short Multi-Cycle Test Plus Steady-State (SMCT+) sequence, as outlined in the SAE J1634 Recommended Practice [4]. Additionally, temperature conditions were varied between standard, 25°C, all the way down to -10°C in several increments to simulate different ambient conditions. Energy consumption and estimated range results were calculated for both vehicles, allowing a rare comparison of the effect of a resistive heater and heat pump on both these metrics.

2.1 Vehicle Specifications

For this test program, two Tesla Model 3s of two different model years were tested on the same drive cycles and at the same temperatures. Vehicle #1 is a model year 2020 and includes the initially offered PTC (resistive) heater for cabin heating. Vehicle #2 is a model year 2022 and includes the advanced heat pump system that is now standard on this vehicle model. General specifications of each vehicle are listed in Table 1. Note that battery capacity was changed between these model years, as well as the drive motors' power outputs, and this is accounted for in the "Percentage Range Retained in Cold Temperatures" section by using the percentage of range retained by each vehicle rather than the absolute range values which vary due to these drivetrain differences.

Table 1: Test Vehicle Specifications

Parameter	Vehicle #1	Vehicle #2
Cabin Heating Type	PTC heater	Heat pump
Refrigerant Type	R134a (for air conditioner)	R1234yf
Make	Tesla	Tesla
Model	Model 3 LR AWD	Model 3 LR AWD
Model Year	2020	2022
Manufacturing Date	01/20	11/21
Curb Weight (lb)	4033	4052
GVWR (lb)	5072	4883
Equivalent Test Weight (lb)	4250	4250
Motor Power Front/Rear (kW) [5]	147/188	98/195
Battery Description	Lithium-ion, NCA cathode	Lithium-ion, NCA cathode
Rated Battery Capacity (kWh)	75 [6]	82 [7]
UBE from Certification (kWh)	79.8 [8]	82.1 [9]
Rated Electric Range (km) [10]	518	576
Rated Energy Consumption (Wh/km) (City/Hwy/Comb) [10]	169/180/174	156/166/160
Tire Make/Model (OEM)	Michelin Primacy	Michelin Primacy
Tire Size	235/45R18	235/45R18
Cold Tire Pressure (psi)	42	42

2.2 Individual Drive Cycles and Daily Test Procedure

2.2.1 Drive Cycles

Standard drive cycles specified in J1634 for the purpose of light-duty vehicle testing were driven during this test program, including the Urban Dynamometer Driving Schedule (UDDS, also known as the LA4) city cycle, the Highway Fuel Economy Test (HWFET) highway cycle, and the US06 aggressive driving cycle (one of the supplemental federal test procedure cycles). A sequence of these cycles was completed at each test temperature (rather than only testing the typical Cold FTP cycle at -7°C) to provide a more detailed view of the performance of each vehicle at different temperatures. The drive cycle traces were followed on the chassis dynamometer by technicians who controlled the vehicle while looking at a driving speed trace on a driver's aid screen.

2.2.2 SMCT+ Procedure

The version of the SAE J1634 procedure published in 2021 includes two test procedures which are intended to reduce the test burden on test facilities, specifically the Short Multi-Cycle Test (SMCT) and Short Multi-Cycle Test Plus Steady-State (SMCT+) procedures [4]. In this case, the SMCT+ procedure was chosen since it does not require the use of a bidirectional charger, which is used for battery depletion during the SMCT and was not available at the testing facility. Instead, the SMCT+ allows battery depletion to be performed on the chassis dynamometer at a steady speed of 65 mph with the appropriate road load simulation active. The SMCT+ also offers test duration and test burden advantages over the original Multi-Cycle Test (MCT) procedure, as the MCT requires an additional steady speed cycle to be driven in the middle of the test sequence. In summary, the SMCT+ was chosen for this program since it offers some of the test duration advantages of the SMCT while allowing the test to proceed using only a chassis dynamometer, like the MCT.

Specifically, the SMCT+ procedure begins with a sequence of seven drive cycles: two repeats of the UDDS, one HWFET, one US06, a second HWFET, and a final two repeats of the UDDS [4]. This sequence is shown in Figure 1. After the test sequence shown, the vehicle was driven at a constant speed of 65 mph until the end of test criterion was met, meaning the battery was depleted. The end of test criterion specifies that the vehicle should be decelerated smoothly to a stop within 15 seconds when it can no longer meet the desired speed (65 mph) to within a 2-mph tolerance [4]. This end of test criterion was followed for all full depletion test days.

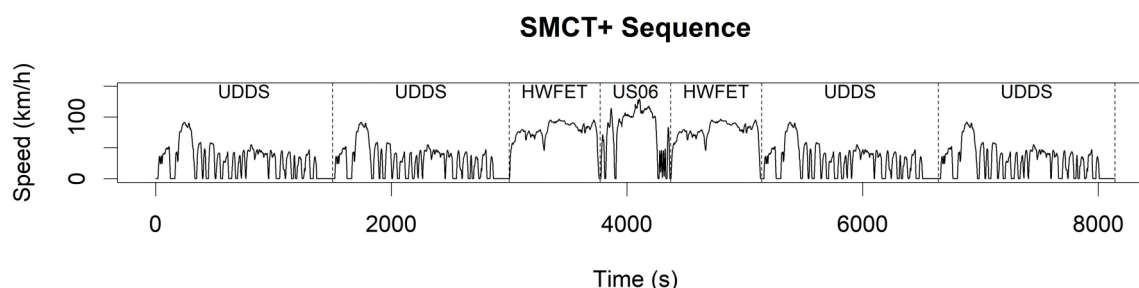


Figure 1: SMCT+ initial drive cycle sequence

Some test days included only the seven initial drive cycles from the SMCT+ procedure, and these were considered “partial depletion” test days. The results of these partial depletion tests were used in the calculation of energy consumption (and driving range, by extension) but could not be included in the calculation of Usable Battery Energy (UBE) because the battery was not fully depleted.

2.3 Test Conditions and Cabin Conditioning

The intent of this test program was to test the vehicles at a range of test temperatures, thus obtaining energy consumption data for a variety of conditions. 25°C was set as the baseline temperature for testing, as this is the standard condition for laboratory testing of vehicles. For this condition, no heating or cabin conditioning of any sort was used. The cold temperatures used to compare to this baseline were 0°C , -7°C (the standard temperature for cold testing), and -10°C . At each of these additional temperatures, the cabin conditioning was set to a 22°C temperature setpoint with automatic fan speed and direction.

2.4 Test Matrix

This test program included some full depletion tests (where the battery of the vehicle was fully depleted at the end of the test) as well as some partial depletion tests (where only the first seven cycles were driven). Every test day, whether full depletion or partial depletion, began with the vehicle having a fully charged battery (as close to 100% State of Charge, or SOC, as the vehicle software would allow).

Table 2: Test Matrix (repeated for each vehicle)

Temperature	25°C	0°C	-7°C	-10°C
Full Depletion Days	1	1	1	1
Partial Depletion Days	2	0	2	0

2.5 Instrumentation

Vehicle #1 (PTC) was tested first for several weeks, and then Vehicle #2 (heat pump) was tested afterward, since instrumentation was shared between the two vehicles. The main instrumentation for this test program consisted of a pair of Hioki PW6001 power analyzers, connected to form a 12-channel power analyzer system. The traction battery voltage signal was read directly from inside the battery penthouse (a compartment on top of the battery pack) and was used as the voltage signal for all high voltage systems. Up to 11 Hioki current probes were used to measure the current from each sub-system within the vehicle (as needed). 208V AC grid current and voltage were also measured during charging only. Table 3 includes a list of the sub-systems that were monitored and the power analyzer setup for each vehicle.

Some of the channels listed for each vehicle in Table 3 are repeated with positive and negative signs noted. This is due to the chosen method of instrumentation, which was required to be as non-invasive as possible for this test program. Since the Hioki current probes (models CT6843 and CT6845-05) are of the clamp-on type, they could be installed directly overtop of the insulated current-carrying cables, without cutting into the wires. However, electric vehicle high voltage system cables also generally include shield wiring around the main current carriers. The currents within these shield wires can cause significant inaccuracy in the measurements if they are not accounted for, and so the “dual probe” method was used to account for this.

The dual probe method consists of installing two probes on each measured system, one probe on the positive cable, and another probe on the negative cable, in opposite directions. With these two probes measuring the same system, and if the shield current is identical in both cables’ shield wiring, the average value of the two current probe readings is the desired measurement (since the shield currents are cancelled out). Note that each sub-system must include two individual voltage cables (positive and negative, not a common negative) to use this method, but must have electrically connected shields. Some Hioki channels did not use this method because their cables were not shielded, including the low voltage DC-DC output and the AC grid connection.

Table 3: Power analyzer instrumentation channels

Ch.	Vehicle 1	Voltage Range (V)	Current Range (A)	Vehicle 2	Voltage Range (V)	Current Range (A)
1	Front Motor (+)	600	500	Front Motor (+)	600	500
2	Front Motor (-)	600	500	Front Motor (-)	600	500
3	Rear Motor (+)	600	500	Rear Motor (+)	600	500
4	Rear Motor (-)	600	500	Rear Motor (-)	600	500
5	DC-DC Input/Main Battery (Charging) (+)	600	20	DC-DC Input/Main Battery (Charging) (+)	600	20/40 (changed)
6	DC-DC Input/Main Battery (Charging) (-)	600	20	DC-DC Input/Main Battery (Charging) (-)	600	20/40
7	A/C Compressor (+)	600	80	N/A	-	-
8	A/C Compressor (-)	600	80	N/A	-	-
9	PTC Heater (+)	600	80	Heat Pump (+)	600	80
10	PTC Heater (-)	600	80	Heat Pump (-)	600	80
11	DC-DC Output	15	200	DC-DC Output	15	200
12	Dyno Speed/AC Grid (Charging)	15/300 (DC/AC)	-/80	Dyno Speed/AC Grid (Charging)	15/300 (DC/AC)	-/80

The “DC-DC Input/Main Battery” and “Dyno Speed/AC Grid (Charging)” channel names are split to denote the fact that they collected different data during driving and charging.

2.6 Calculations

2.6.1 Energy Consumption

Component energy for this vehicle was captured and reported by the Hioki power analyzers during each drive cycle driven on the chassis dynamometer. The DC energy sent from the battery to each component was added together to make a total DC battery energy value in Watt-hours (Wh) for each test (denoted as E_{DC}). The DC energy consumption in Wh/km was calculated by dividing this value by the distance driven (D) in km for the corresponding test, as shown in Equation (1).

$$EC_{DC} = \frac{E_{DC}}{D} \quad (1)$$

2.6.2 J1634 Combined Energy Consumption Calculation

The SAE J1634 Recommended Practice includes calculations to combine the results of each individual drive cycle during an SMCT+ test day into a composite energy consumption value for each cycle type (i.e. for the UDDS, HWFET, and US06 cycles) using “Phase Scaling Factors” (denoted as “k” in equations) [4]. For the UDDS cycle, this allows the cold start effect to be reduced, to make the energy consumption and range results more comparable to the other cycles that do not have as pronounced a cold start effect. The calculations for the UDDS cycle energy consumption in Wh/km are shown in Equation (2). For the HWFET and US06 cycles, the Phase Scaling Factors (k) equal one divided by the number of cycles of each type, so the final values end up being equivalent to the average energy consumption during all of that particular type of cycle on that test day (for the US06, there is only one test cycle so the value for that one is taken as the final daily value).

$$EC_{DC\ UDDS} = \sum_{i=1}^4 k_i * EC_{DC\ UDDS_i} \quad (2)$$

where $k_1 = \frac{E_{DC\ UDDS_1}}{E_{DC\ Total}}$
and $k_{2,3,4} = \frac{1-k_1}{3}$

2.6.3 Driving Range Estimation

The Usable Battery Energy (UBE) in Wh was calculated by taking the summation of all the total DC battery energy (E_{DC}) values for each drive cycle on a particular day. Only one full depletion test was completed at each temperature for each vehicle to obtain this UBE. Then, to obtain the estimated driving range in km for a particular cycle, this UBE in Wh was divided by the cycle-specific combined DC energy consumption ($EC_{DC\ cycle}$) in Wh/km, as shown in Equation (3).

$$Range_{calc} = \frac{UBE}{EC_{DC\ cycle}} \quad (3)$$

3 Results

3.1 Cabin Heating Loads

One way to analyze the cabin heating performance of the test vehicles is to compare the average load required by the heating system of each vehicle. Looking at the power, or load, demanded by each system rather than its energy consumption removes the effect of the selected drive cycle trace on heating system performance and allows comparison between heating loads during disparate cycles and over the course of the full test day. The average cabin heating loads during each of the drive cycles performed by each vehicle on each test day are illustrated in Figure 2 (note that the 25°C temperature results are not shown because they are zero since the heating systems were turned off). The cycles in this graph are separated by their driven order during the day and are denoted using two numbers referring to their “round” and “mode”. “Round” refers to each sequence of tests that were loaded into the test computer (for example, round 1 consists of two repeats of the UDDS cycle in quick succession). “Mode” refers to the drive cycle’s order within its round, for example “1-2 UDDS” refers to mode 2 of round 1, the second cycle of the first round of testing, and the second cycle driven overall.

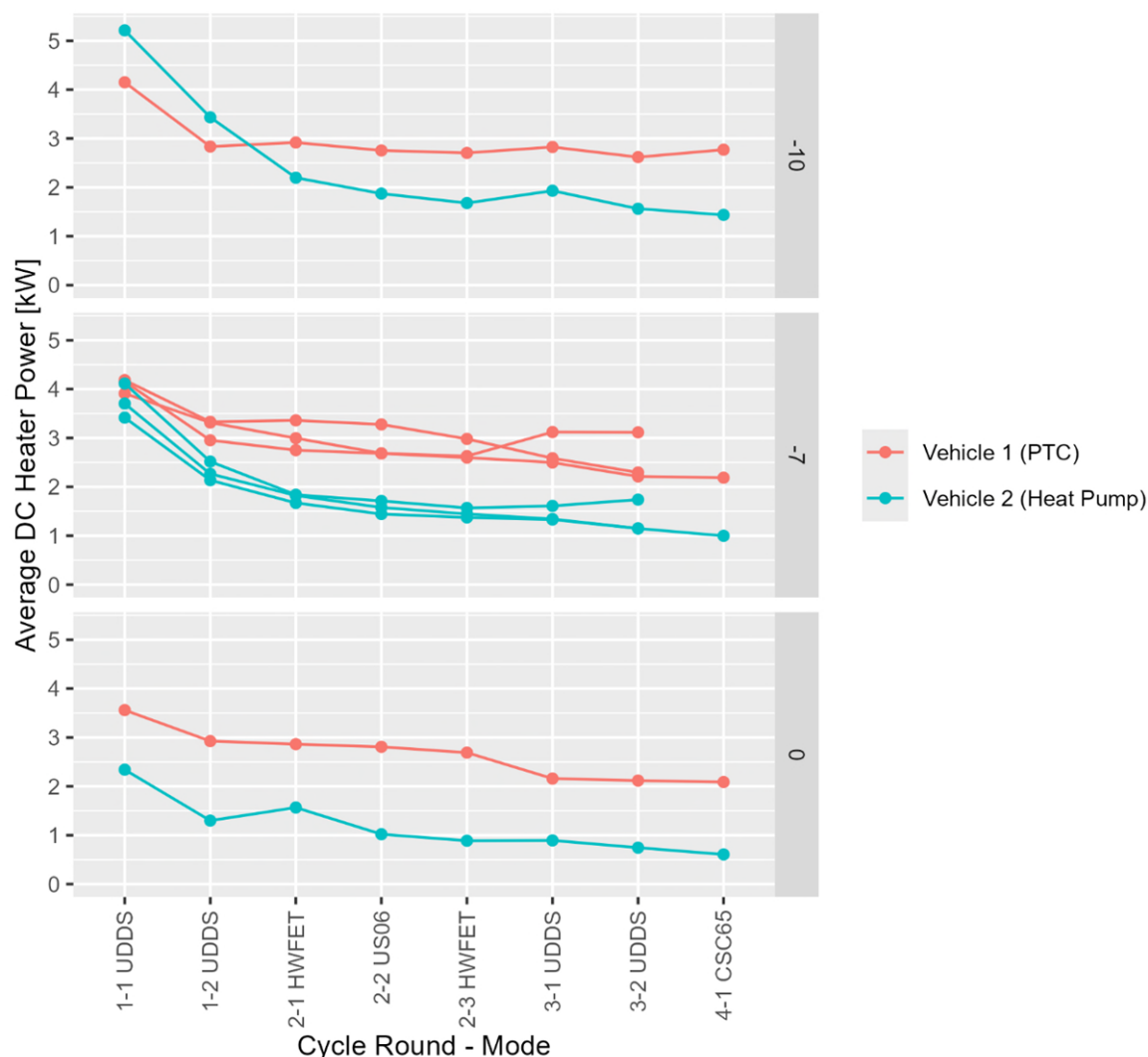


Figure 2: Average cabin heating loads at different temperatures for each vehicle and test type/day by Round and Mode (note heating load at 25°C is not shown because it was zero)

For both vehicles, the heating load was highest in the first (cold start) cycle of the test day, as the vehicles were soaked at the ambient test temperature and the heating systems had to increase the cabin temperature significantly to reach the 22°C setpoint. Subsequent tests showed lower heating loads as the cabin was already warmed up prior to the start of these cycles, because of heater use during the preceding tests. Pre-heating the vehicles could mitigate some of the cold start effect on heating load (and therefore on energy consumption and vehicle range as well), however pre-heating was not included in this test program.

The heat pump equipped vehicle (Vehicle 2) generally required a lower average cabin heating load than the PTC heater equipped vehicle (Vehicle 1), except on cold start at the coldest conditions (-10°C and -7°C). At -10°C, the heat pump equipped vehicle had a higher cabin heating load than the resistive heater equipped vehicle for the first two test cycles of the day. At -7°C, the heating loads were similar for both vehicles on the first test of the day. For all other tests, Vehicle 2 (equipped with the heat pump) showed lower average heating power. The reason for this reversal of heating load at very cold temperatures could be due to “lossy mode” operation of the heat pump, where it can be used to create heat directly from electrical energy and not to efficiently transfer heat from the surroundings to the cabin [2, 3]. In this lossy mode, the energy use of the heat pump appears to have been greater than that of the simple PTC heater, perhaps due to the additional steps required to transfer the heat first through the refrigerant, then to the coolant system through a chiller, and then to the cabin [3].

Comparing all test days, the heat pump showed the greatest efficiency advantage over the PTC heater at a

moderately cold temperature of 0°C, using less than half the average power of the PTC heater on many cycles at that temperature. At -7°C and -10°C, the heat pump advantage was low (and, as mentioned, became a disadvantage at -10°C) upon cold start, but improved as the test days progressed. Over longer drives at these temperatures, this advantage would be helpful to increase the vehicle's driving range once the cabin reached its setpoint temperature. The next several sections include the effect of these differing heating loads and temperatures on component and vehicle energy consumption, as well as the calculated driving range of the vehicles over the different test cycles.

3.2 Component-Level Energy Consumption

Since each high voltage component or system on the vehicles was measured independently using the power analyzers, the energy consumption of each vehicle can be broken down as component-level energy consumption, as shown in Figure 3. The total height of each bar in this figure represents the total energy consumption for the vehicle at that test condition (temperature and test cycle, including sequence during the day). Each bar is further broken down into motor/inverter energy consumption in its bottom section, accessory (DC-DC converter) energy consumption in its middle section, and cabin heating, ventilation, and air conditioning (HVAC) energy consumption in its top section. Where available, multiple test repeats were included in these values and the average value is shown (multiple tests were available for temperatures of 25°C and -7°C only). Each test cycle is shown in its proper sequence during the test day with numbering pertaining to its "round" and "mode" within the test sequence.

Similarly to the heating loads shown in Figure 2, the heating (HVAC) energy consumption values shown in Figure 3 were significantly higher during the first drive cycle of each day than in subsequent cycles, and were sometimes high for the second drive cycle of the day as well. However, the effect of the driving cycle is also apparent in Figure 3: even though the heating loads of different test cycle types (after the cold start) may have been similar in Figure 2, their effect on energy consumption could be very different due to the test cycle. Generally, the effect of heating loads on cycles with higher average speeds (HWFET, US06, and CSC cycles) is lower than on the city-type cycle with lower average speeds (UDDS). This is because over a similar test duration, heating energy will be divided by a larger distance in its energy consumption calculation if the average vehicle speed of the vehicle was higher, leading to a lower energy consumption value for a similar heating load. This effect also means that the calculated vehicle ranges over the higher speed cycles are less affected by heating loads than those over the UDDS cycle, which is evident in the results in the "Calculated Driving Range" and "Percentage Range Retained" sections of this report.

Accessory energy consumption (which was measured at the input to the DC-DC converter) was affected by cycle speed in the same way as HVAC energy consumption. In general, however, the accessory energy consumption was much lower in magnitude than the heating energy consumption, as shown in Figure 3 (except during 25°C testing, which had no HVAC component). Accessory energy consumption also did not vary as significantly due to temperature or cold start conditions. The lowest accessory energy consumption was recorded during 25°C testing, potentially due to the lack of cabin heating fan usage.

The motor/inverter energy consumption shown in Figure 3 also varied significantly due to cold start condition, temperature, and cycle type. A portion of this motor/inverter energy consumed may have been used to heat the vehicles' batteries during cold temperatures. This is a feature of this vehicle model and unfortunately the motor/inverter energy used to heat the battery could not be broken out from the overall motor/inverter energy consumption. Cold temperatures also generally increase tire and drivetrain losses in vehicles, and this is accounted for in the motor/inverter energy consumption.

The lowest motor/inverter energy consumption was recorded over the UDDS cycle, which features light accelerations rates and low average speeds, along with lots of opportunity for regenerative braking during deceleration. The highway (HWFET) cycle also had relatively low motor/inverter energy consumption due to its moderate speeds and lack of heavy acceleration. The US06 cycle, which is considered to contain aggressive driving, had the highest motor/inverter energy consumption, except at cold temperatures where cold start effects dominated during the cold start UDDS cycle (as mentioned, this could partly be due to the motor/inverter being used to heat the battery).

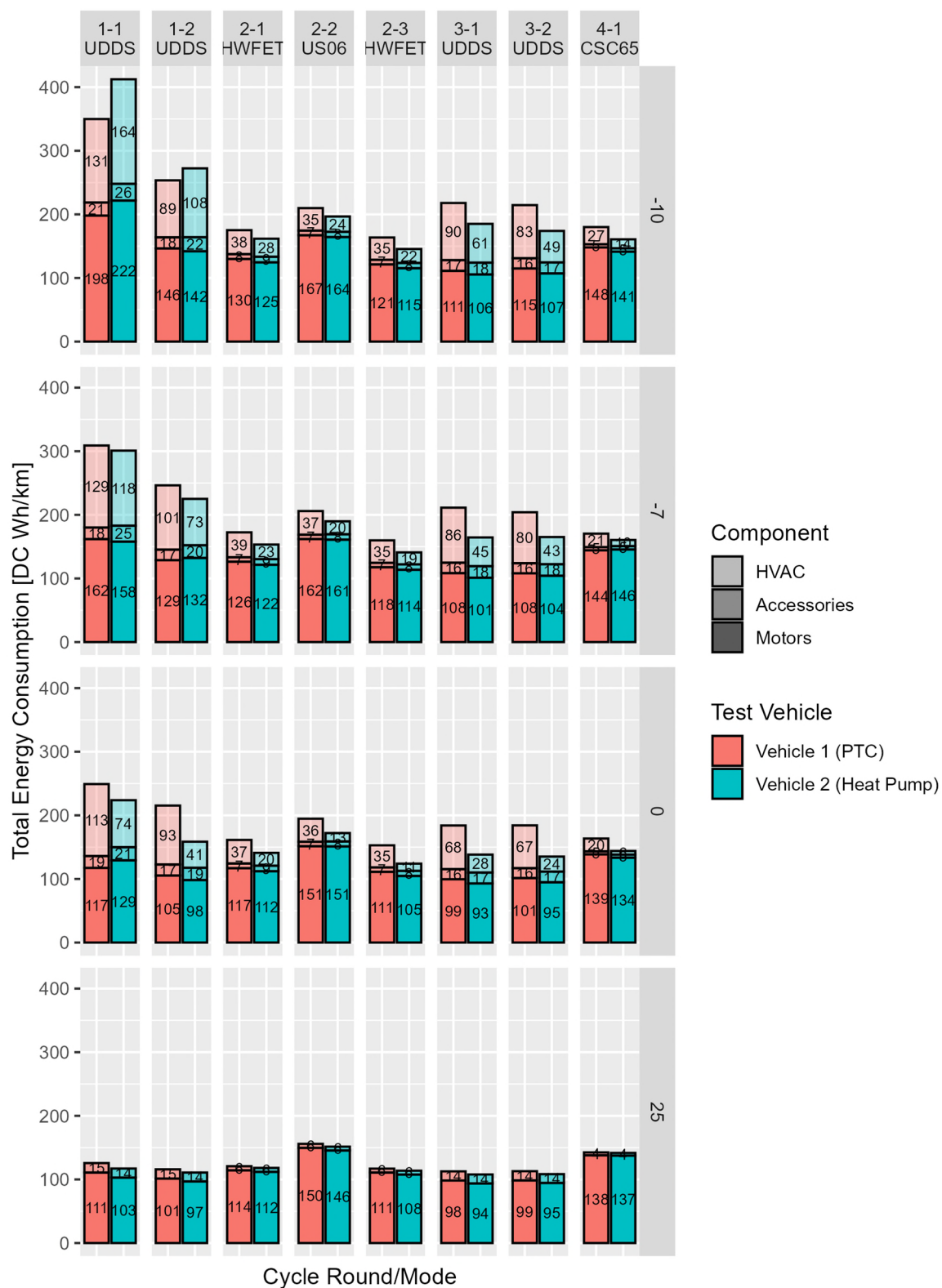


Figure 3: Energy Consumption in Wh/km by cycle, round/mode, temperature, vehicle, and component

3.3 DC Energy Consumption by Drive Cycle

The SAE J1634 Recommended Practice for testing battery electric vehicles includes calculations to convert the energy consumption over individual test cycles driven during the SMCT+ test sequence into composite values for each type of drive cycle (UDDS, HWFET, and US06) [4]. This requires the use of a “Phase Scaling Factor”, which lowers the cold-start effect on UDDS energy consumption, as explained in the “J1634 Combined Energy Consumption Calculation” section. The composite results for the other two types of test cycle are essentially the average values for each of those cycle types during each day. Figure 4 shows the J1634-calculated combined DC energy consumption values for each vehicle, test temperature, and drive cycle type (except for the CSC, as it is not a standard compliance cycle). These DC energy consumption values along with UBE are later used to calculate range.

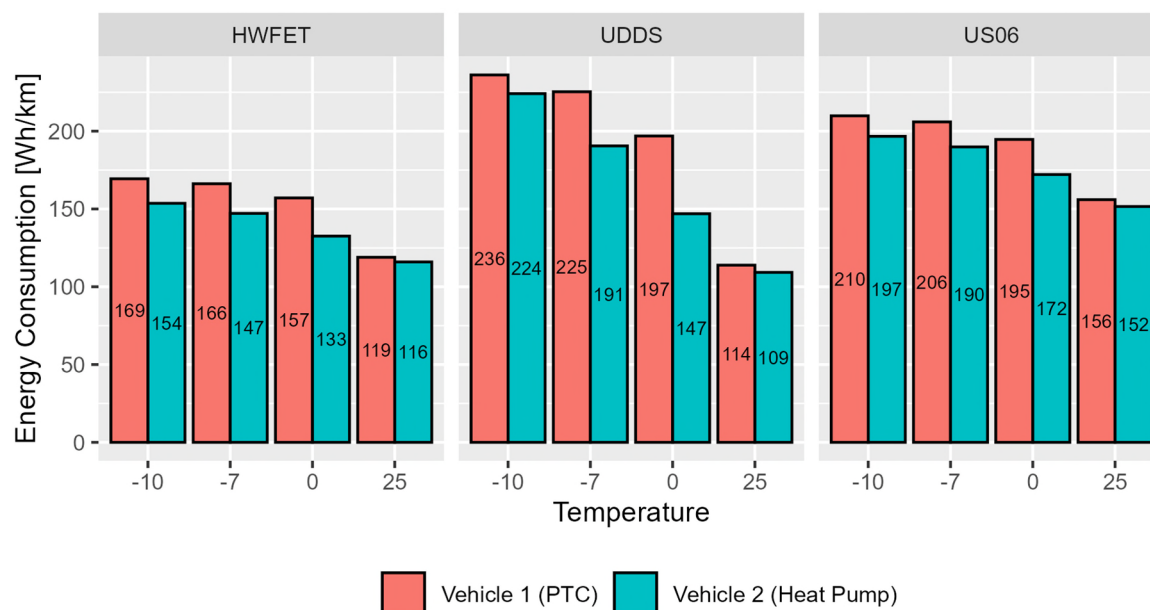


Figure 4: J1634 Combined DC Energy Consumption by drive cycle and temperature for each vehicle

Figure 4 shows the largest temperature effects on energy consumption occurred during the UDDS cycle, with the UDDS energy consumption at -10°C for both vehicles being over twice that of their respective UDDS energy consumption at 25°C. As mentioned in previous sections, this is due to cold start effects on the heating and drivetrain systems, as well as increased heating loads in general at cold temperatures, combined with the low average speed of the UDDS cycle. Since these are composite values and the cold start effects are reduced, the heat pump equipped vehicle (Vehicle #2) managed to obtain lower energy consumption than Vehicle #1 over all composite cycle results and temperatures (even though it had higher energy consumption over the first two UDDS cycles at -10°C, as shown in Figure 3, this was overcome by its advantage during the other two UDDS cycles at that temperature). The improved energy consumption due to the heat pump was most apparent at 0°C over the UDDS and HWFET cycles. The improvement in efficiency for Vehicle #2 is also obvious at -7°C over the UDDS cycle and at 0°C over the US06 cycle, among others.

3.4 Usable Battery Energy

Figure 5 shows the recorded UBE for each completed full-depletion test at each temperature and for each test vehicle. As shown in Table 1, the UBE for Vehicle #1 was expected to be slightly lower than that of Vehicle #2. At 25°C, the vehicles reached their highest UBE values, however neither vehicle reached its UBE reported during certification at this temperature (potentially due to battery degradation). The UBE of electric vehicles is generally reduced at low temperature due to temperatures effect on the Li-ion batteries [11]. This was true for both test vehicles in this study, with their highest UBE values both being recorded at 25°C. Uncharacteristically, the lowest UBE for Vehicle #2 was recorded at a moderate 0°C, and UBE at -7°C was higher than the UBE at 0°C for both test vehicles. This may partly be explained by inter-test variability, as UBE was recorded only once at each test temperature for each vehicle (8 full-depletion tests in total).

The UBE values shown in Figure 5 were used as part of the calculation of the vehicles' ranges over the test cycles at different temperatures, and the effect of reduced UBE at cold temperatures is included alongside that of increased energy consumption due to cabin heating in the "Calculated Driving Range" and "Percentage Range Retained" sections.

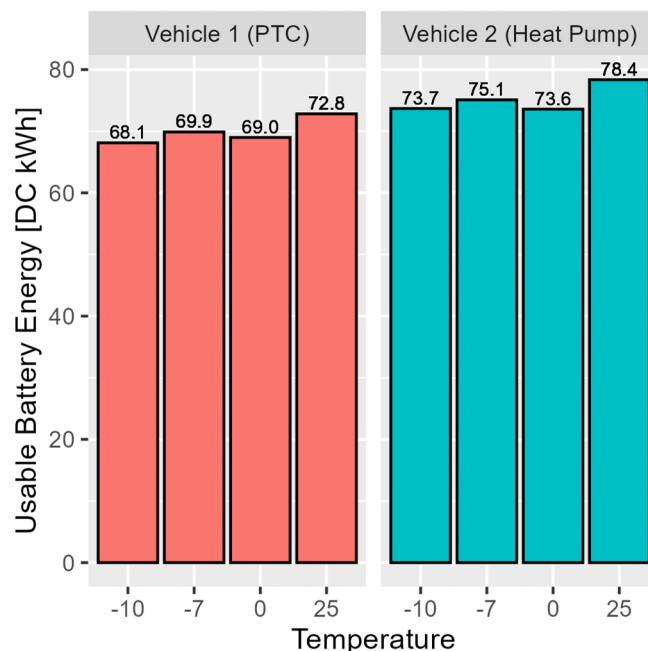


Figure 5: Usable Battery Energy of both test vehicles during full depletion tests at different temperatures

3.5 Calculated Driving Range by Drive Cycle

Using the methods described in the "Driving Range Estimation" section, the authors determined an estimated driving range for each test cycle at each test temperature, as shown in Figure 6. Combining both the UBE and the DC energy consumption values from previous sections (as they would be in real world cold temperature conditions), the driving range for each cycle type and temperature was calculated for both vehicles. Since Vehicle #2 has a slightly larger battery capacity than vehicle #1, its range was consistently higher than that of Vehicle #1. However, the intent of this project is to characterize the effect of heating systems on vehicle energy consumption and range, so the differences in range between temperature conditions for each vehicle individually are the key takeaways from Figure 6.

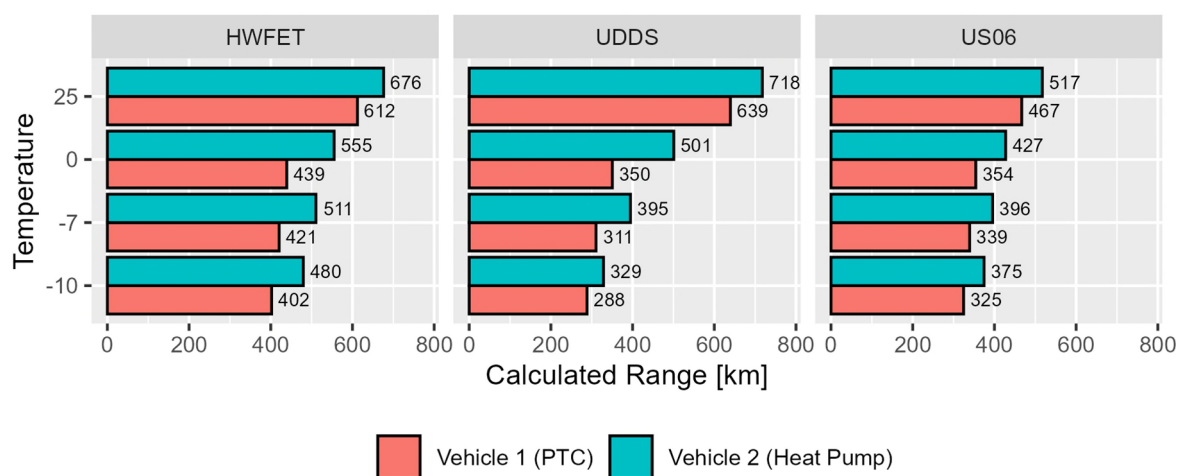


Figure 6: Calculated vehicle range for each cycle and temperature, J1634 phase-scaling factors applied.

The results shown in Figure 6 reveal significant range reductions for both vehicles at cold temperatures, especially over the UDDS cycle. The UDDS cycle range is particularly affected by heating in cold temperatures because of its low average speed, leading to high heating energy consumption per unit distance and a more than 50% reduction in driving range at the coldest temperature when compared to 25°C. Conversely, the maximum range of each vehicle was achieved over the UDDS cycle in 25°C temperatures, since this cycle has relatively gentle accelerations and has low average speeds (leading to low aerodynamic drag losses and low drivetrain energy consumption).

The maximum range of the vehicles at 25°C was lowest over the US06 cycle, owing to its aggressive accelerations and high-speed driving. However, at the coldest temperatures, the vehicles achieved a higher calculated range on the US06 than on the UDDS cycle due to the less pronounced effect of cabin heating over the higher speed cycle. The HWFET results showed the longest ranges for both vehicles at any temperature except 25°C, since heating energy consumption values were low due to its high average speeds, and because the HWFET driving cycle is more moderate in both speeds and acceleration rates than the US06.

For BEV range purposes, ratings agencies combine the UDDS and HWFET ranges obtained during testing of different drive cycles (using a 55% and 45% weighted average value) and then multiply this computed value by an “adjustment factor” to better estimate real-world performance. Vehicle manufacturers can either use the standard 2-cycle adjustment factor of 0.7 or calculate a 5-cycle adjustment factor. In this case, high temperature (35°C) testing was not performed on either vehicle, so calculation of their 5-cycle adjustment factors could not be completed. Therefore, the factors from certification documents were used instead. Combining the UDDS and HWFET range values at 25°C with their appropriate weightings and applying the certification adjustment factor for each vehicle (0.70 for Vehicle #1 and 0.73 for Vehicle #2), we obtain range ratings of 441 km and 510 km for Vehicle #1 and Vehicle #2, respectively, based on our chassis dynamometer testing. These values are lower than the vehicles’ rated ranges (518 and 576 km, respectively). This is due to the lower UBE values for both vehicles (which could be due to battery degradation and test procedure differences) and higher vehicle energy consumption when compared to certification results (which may be due to the laboratory test setup/loading).

The next section shows a method to directly compare the two vehicles and their heating systems using the percentage of range retained rather than the absolute calculated range of each vehicle.

3.6 Percentage Range Retained in Cold Temperatures

It is informative to look at the range retained as a percentage of the maximum range for each cycle and vehicle, as illustrated in Figure 7. This allows a direct comparison of the range retained by the two vehicles at different temperatures over different cycles. In this graph, each bar represents the associated vehicle’s expected range at different temperatures, as a percentage of its own maximum range over that cycle at 25°C. This removes the effect of the difference in battery capacity between the vehicles, although differences in the percentage of each vehicle’s UBE retained at different temperatures are still included in these results.

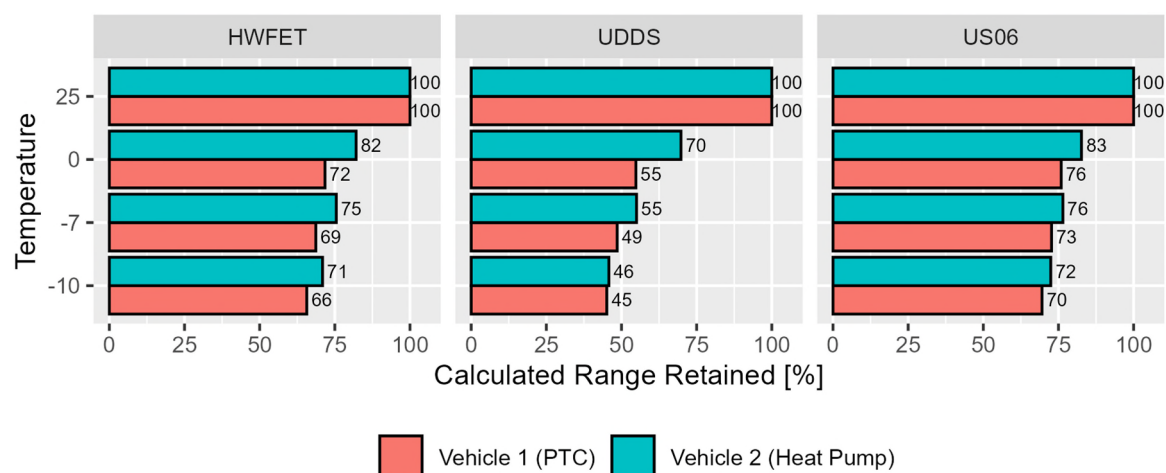


Figure 7: Estimated Driving Range Retained over different Cycles at different Temperature, by Vehicle, J1634 Scaling Factors Applied, Normalized to the highest value for each Vehicle and Cycle

Figure 7 reveals that the improved range retention capability of the heat pump is highest at 0°C, increasing the percentage of retained range by 15% over the PTC heater equipped vehicle on the UDDS cycle, by 10% over the HWFET cycle, and by 7% over the US06 cycle at this temperature. At the two coldest temperatures, the range retention of the vehicle equipped with the heat pump is between 1% and 5% greater than that of the vehicle with the resistive heater. The average benefit of the heat pump equipped vehicle over the PTC heater equipped vehicle was 7% over the UDDS, 7% over the HWFET, and 4% over the US06 cycles over all cold temperatures combined. This level of improvement in range retention is modest but still significant for electric vehicle users in cold climates, where range loss in the cold can be a significant barrier to BEV adoption. Whether adding a heat pump system is a justifiable upgrade to a vehicle depends on the cost of the system and customer requirements for winter driving. In colder climates like in Canada, many new BEVs are now either equipped with a heat pump as standard equipment or have one as an optional range extending heating system for cold weather.

4 Discussion

The heat pump equipped BEV generally achieved lower cabin heating energy consumption and better range retention at low temperatures than the BEV with the PTC heater. However, certain conditions (cold start at -10°C) favoured the PTC heater. Additional testing at temperatures colder than -10°C was not possible at this facility. This vehicle's implementation of a heat pump solution also did not include a backup PTC heater for extreme cold temperatures (likely due to cost), whereas many BEVs do include a PTC heater in addition to a heat pump. A backup PTC heater may have helped improve performance at the coldest temperatures.

Pre-heating the cabin while plugged in to the AC grid and prior to driving each vehicle would lead to reduced heating energy demand for the cold start cycles, increasing driving range. This action was not included in this test program but could be used as a strategy for increasing cold weather BEV range in the real world.

Alternative cabin heating solutions have also been proposed for the BEV market, but none have been widely commercialized. Phase-change materials and radiant heating solutions have been proposed by researchers and manufacturers [12, 13]. Alternative refrigerants have also been proposed for use in electric vehicle heat pump systems, such as carbon dioxide (CO₂), known in industry as R744, and propane, known as R290. Using carbon dioxide refrigerant in heat pump systems has been shown to improve heating performance at very cold temperatures (with a potential reduction in efficiency for cooling) [14]. Another benefit of both CO₂ and propane as refrigerants is that they do not contain persistent chemicals (R1234yf, which is currently widely used in the automotive industry, is suspected to be a source of persistent chemicals) [15].

In the long term, additional charging infrastructure may alleviate some of the importance of maintaining range at cold temperatures. However, the efficiency benefits of heat pump systems from an electricity use and greenhouse gas perspective will continue to be important, even if driving range retention becomes less of a concern due to these improvements in charging infrastructure.

5 Conclusion

Several observations can be drawn from the results of this test program, and are listed in point form below:

- As expected, heating loads were very high on cold start at low temperatures, between 4 and 5 kW throughout the cold start UDDS cycles at the lowest temperatures.
- Unexpectedly, the heat pump system used more power than the PTC heater over the first two drive cycles at the coldest test temperature (-10°C). This may be due to the use of a so-called “lossy” mode of operation that the heat pump can use when high heat is required at low temperatures, which allows the heat pump compressor to produce heat directly from stored electricity but lowers its efficiency significantly. A backup PTC heater may improve this performance at extremely cold temperature.
- The value of the heating component of energy consumption at cold temperatures was highly dependent on the drive cycle; cycles with higher average speeds (HWFET, US06) led to reduced heating energy consumption while cycles with lower average speeds (UDDS) led to increased energy consumption for similar levels of average heating power.
- Overall, the heat pump reduced energy consumption for all drive cycle types at all temperatures when using J1634-type calculations to obtain a single energy consumption result for each drive cycle.

- Calculated range reduction at very cold temperatures was over 50% when compared to standard temperature (25°C) on the UDDS cycle
- Neither vehicle achieved its rated driving range at 25°C (when using their certification adjustment factors and combining UDDS and HWFET results at 55% and 45%, respectively), this may be due to differences in test conditions/loading and battery degradation in the test vehicles.
- The improvement in range retention over the baseline PTC heater system when using the heat pump system varied between 1% and 15%, depending on cycle and temperature
 - o The heat pump achieved the most advantage (15%) at moderate cold temperature (0°C) over the UDDS cycle
 - o At the coldest condition (-10°C) over the UDDS cycle, the heat pump only achieved a 1% advantage overall
- On average, the heat pump equipped vehicle achieved a 7% range retention advantage on the UDDS cycle, 7% on the HWFET, and 4% on the US06 over the PTC equipped vehicle. This amount of improvement in cold temperatures may be beneficial to users in cold climates, and heat pump systems are already available on many BEVs in Canada.

Acknowledgments

The authors would like to thank the staff of Transport Canada's ecoTechnology for Vehicles program for providing the vehicles used in this test program, as well as the staff of the Transportation Emissions and Electrification Laboratory at Environment and Climate Change Canada for performing the testing described in this report. Special thanks to Maurice Osborne, Lukasz Sikorski, and Hussein Rashid of Environment and Climate Change Canada.

References

- [1] Y. Higuchi, H. Kobayashi, Z. Shan, M. Kuwahara, Y. Endo and Y. Nakajima, "Efficient Heat Pump System for PHEV/BEV," *SAE Technical Paper*, 2017.
- [2] N. Mancini, J. S. M. Mardall, J. Koplitz, C. R. O'Donnell, D. F. Hanks and H. Li, "Optimal source electric vehicle heat pump with extreme temperature heating capability and efficient thermal preconditioning". United States Patent 10,967,702, 6 April 2021.
- [3] WeberAuto, "Understanding Tesla's Heat Pump System (Youtube)," 22 May 2023. [Online]. Available: <https://www.youtube.com/watch?v=Dujr3DRkpDU>. [Accessed 15 April 2025].
- [4] SAE International, *SAE J1634 - Battery Electric Vehicle Energy Consumption and Range Test Procedure*, 2021.
- [5] U.S. Department of Energy, "www.fueleconomy.gov," [Online]. Available: www.fueleconomy.gov. [Accessed 17 April 2025].
- [6] Car and Driver, "2020 Tesla Model 3 Long Range AWD Features and Specs," [Online]. Available: https://www.caranddriver.com/tesla/model-3/specs/2020/tesla_model-3_tesla-model-3_2020/412468. [Accessed 24 April 2025].
- [7] Car and Driver, "2022 Tesla Model 3 Long Range AWD Features and Specs," [Online]. Available: https://www.caranddriver.com/tesla/model-3/specs/2022/tesla_model-3_tesla-model-3_2022/426156. [Accessed 24 April 2025].
- [8] United States Environmental Protection Agency, "Application for TESLA, INC. 2020 model year test group LTSLV00.0L23 (Update)," 27 October 2019. [Online]. Available: https://dis.epa.gov/otaqpub/display_file.jsp?docid=48711&flag=1. [Accessed 24 April 2025].
- [9] United States Environmental Protection Agency, "Application for TESLA, INC. 2022 model year test group NTSLV00.0L23," 23 September 2021. [Online]. Available: https://dis.epa.gov/otaqpub/display_file.jsp?docid=54290&flag=1. [Accessed 24 April 2025].
- [10] Natural Resources Canada, "Fuel consumption ratings search tool," Natural Resources Canada, [Online]. Available: <https://fcr-ccc.nrcan-rncan.gc.ca/en/>. [Accessed 2 February 2020].
- [11] J. Jaguemont, L. Boulon and Y. Dubé, "A comprehensive review of lithium-ion batteries used in hybrid and electric vehicles at cold temperatures," *Applied Energy*, vol. 164, pp. 99-114, 2016.

- [12] P. Weissler, "Electric radiant heat for EV cabin comfort," 19 May 2022. [Online]. Available: <https://www.sae.org/news/2022/05/electric-radiant-heat-for-ev-cabin-comfort>. [Accessed 9 April 2025].
- [13] E. Mandev, M. Akif Ceviz, F. Afshari and B. Muratçobanoğlu, "Evaluating PCM heat battery as a range-saving solution for electric vehicle cabin heating," *Sustainable Energy Technologies and Assessments*, vol. 76, no. 2213-1388, 2025.
- [14] C. Liu, Y. Zhang, T. Gao, J. Shi, J. Chen, T. Wang and L. Pan, "Performance evaluation of propane heat pump system for electric vehicle in cold climate," *International Journal of Refrigeration*, vol. 95, no. 0140-7007, pp. 51-60, 2018.
- [15] J. Motavalli, "Inside the quiet, never-ending battle over automotive refrigerants," 1 November 2024. [Online]. Available: <https://www.sae.org/news/2024/11/refrigerant-fight>. [Accessed 9 April 2025].
- [16] M. P. O'Keefe, A. Simpson and K. J. Kelly, "Duty Cycle Characterization and Evaluation Towards Heavy Hybrid Vehicle Applications," in *SAE World Congress and Exhibition*, Detroit, Michigan, 2007.
- [17] A. J. Edwards, "Aggressive-dynamics metrics for drive-cycle characterization," *Transportation Research Interdisciplinary Perspectives*, vol. 14, no. 2590-1982, p. 100592, 2022.

Presenter Biography



Aaron Loiselle-Lapointe is a Senior Project Engineer with the Transportation Emissions and Electrification Laboratory at Environment and Climate Change Canada, where has conducted electric vehicle test programs for more than 12 years. Aaron contributes to international working groups, regulatory developments and investigative studies to better characterize the effects of numerous variables on vehicle-level performance metrics. Aaron holds a Master of Applied Science degree in the field of Environmental Engineering and a Bachelor of Engineering degree in Aerospace Engineering from Carleton University.